applied optics

Determination of size and complex index of refraction of single particles with elastic light scattering

MIR SELIMAN WAEZ,[1] STEVEN J. ECKELS,[2] AND CHRISTOPHER M. SORENSEN[3,*]

[1]Powertrain Engineering Division, Southwest Research Institute, San Antonio, Texas 78238, USA
[2]Institute for Environmental Research (IER), Department of Mechanical and Nuclear Engineering, Kansas State University (KSU), Manhattan, Kansas 66506, USA
[3]Department of Physics, Kansas State University, Manhattan, Kansas 66506, USA
*Corresponding author: sor@phys.ksu.edu

Received 30 October 2020; revised 14 December 2020; accepted 15 December 2020; posted 16 December 2020 (Doc. ID 413675); published 14 January 2021

We show that for spherical particles greater than ca. 5 μm, the differential scattering cross section is only weakly dependent on the real and imaginary parts of the refractive index ($m = n + i\kappa$) when integrated over angle ranges near $37 \pm 5°$ and $115 \pm 5°$, respectively. With this knowledge, we set up an arrangement that collects scattered light in the ranges $37 \pm 5°$, $115 \pm 5°$, and $80 \pm 5°$. The weak functionality on refractive index for the first two angle ranges simplifies the inversion of scattering to the particle properties of diameter and the real and imaginary refractive indices. Our setup also uses a diamond-shaped incident beam profile that allows us to determine when a particle went through the exact center of the beam. Application of our setup to droplets of an absorbing liquid successfully determined the diameter and complex refractive index to accuracies ranging from a few to ten percent. Comparisons to simulated data derived from the Mie equations yielded similar results.

https://doi.org/10.1364/AO.413675

1. INTRODUCTION

The purpose of this paper is to demonstrate regimes of weak refractive index functionality in the differential cross section for large, homogeneous spherical particles. We then describe a new method to use elastic light scattering to measure the fundamental particle properties of size and both parts of the complex index of refraction for large, homogeneous, spherical particles. Our method applies to single particle detection. This lays the foundation for construction of a simple device to measure these fundamental properties.

For spheres, the Mie equations solve the so-called "forward problem" of light scattering, which is to calculate the angular scattering pattern given the spherical particle size, R, and complex refractive index, $m = n + i\kappa$ [1]. On the other hand, the solution of the light-scattering "inverse problem," which is to determine the three particle properties R, n, and κ given the measured scattering pattern, is ambiguous, "ill-posed", and hence difficult. Nevertheless, significant attempts have been made to solve the inverse problem for spheres. For example, Eidhammer *et al*. [2] described the end development of a twin-angle optical particle counter (OPC) for micrometer-sized spherical particles that used a white light source. The scattering was detected at $40° \pm 7°$ and $74° \pm 9.2°$ to determine particle size and complex refractive index. A multi-angle, aerosol spectrometer probe (MASP) that was developed by Baumgardner *et al*. [3] collected the scattered light from each particle passing through a focused laser beam over two discrete regions of forward (30°–60°) and backward (120°–150°) scattering angles. The MASP could measure spherical particle size in the range 0.4–10 μm and real refractive index between $n = 1.30 - 1.60$. Hu *et al*. [4] describe a detector to collect light scattered at 60° and 90° each, with a semi-angle range of 20°. This device was capable of measuring size and the complex refractive index. Szymanski and coworkers [5,6] designed and built a dual-wavelength optical particle spectrometer (DWOPS). The device used two different wavelengths and collected light scattered from single particles over the angular ranges 10° to 30° and 150° to 170°. Retrieval accuracies of ∼10% for size and ∼15% for the refractive indices were obtained for spheres in the size range 0.1 to 10 μm.

These successful devices share characteristics of detecting light scattered at two different angles over a broad range of angles and, in some cases, using more than one wavelength. Following the observation of Eidhammer *et al*., these characteristics tend to integrate out the oscillations in the scattering, the ripple structure, to create a more monotonic functionality of the

scattering with the three primary properties of R, n, and κ. This in turn makes the inverse scattering problem less problematic.

Detection and characterization of supra-micrometer particles is important in both atmospheric and aqueous environments. For aerosols, these are often referred to as coarse-mode particles. They occur as dusts such as wind-blown mineral dusts, which represent the largest mass fraction of aerosols in the Earth's atmosphere, grain and coal dusts, bio-aerosols, indoor cooking aerosols, large combustion particles from wildfires, and volcanic ash. Of course, most of these particles are neither spherical nor homogeneous. However, some measurement, with proper caveats, is better than no measurement at all. Moreover, we have reason to believe that the results we will report here will provide a foundation for future research, using our approach, that will lead to some success for measurement of these properties for any particle morphology. Finally, we remark that determination of complex index of refraction provides a good indication of the composition of particulates.

In this work, we demonstrate two special angles near 37° and 115°, where the differential scattering cross section for large, homogeneous, spherical particles is either independent of, or shows a weak functionality on, the real part, n, and the imaginary part of the refractive index, κ, respectively. We call these angles "stationary angles". These stationary angles actually require integration over a small range of a few to several degrees. Measurement of light scattered at these two stationary angle ranges are then functions of R and κ, or R and n, respectively. This simple delimitation of variables, when combined with a measurement at a third angle where the scattering contains information about all three primary properties, leads to an economical solution for all three primary properties, R, n, and κ. This work is an extension of previous work, where it was shown that particles could be sized independently of their real refractive indices with optical detections at ±37° scattering angle [7]. Here, we add the second stationary angle unknown to us at that time.

We limit this work to spheres. Calculations for non-spherical particles are more labor-intensive and will be pursued in the future. Nevertheless, it is worthwhile to note that non-spherical particle light scattering has many properties semi-quantitatively similar to those of the sphere regime as uncovered by Q-space analysis [8].

2. STATIONARY ANGLES

Our goal is to describe a method to simultaneously measure spherical particle size, R, and the complex refractive index, $m = n + i\kappa$. To do this, it is important to realize that the imaginary part of the refractive index, κ, does not directly affect scattering and absorption, but instead its effect is quantitatively described through the relative skin depth parameter, κkR [9–11], *viz.*

$$\kappa kR = R/\delta. \tag{1}$$

In Eq. (1), $k = 2\pi/\lambda$, where λ is the wavelength of light and δ is the $1/e$ penetration depth of the optical field. The effects of κ are nil or barely noticeable when $\kappa < 0.1$, and saturate when $\kappa kR > 3$.

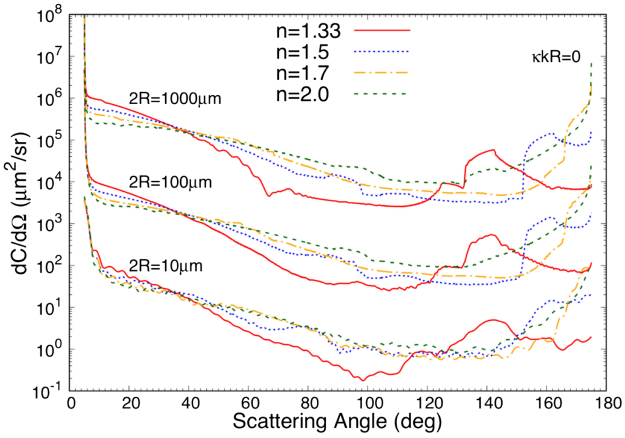

Fig. 1. Light scattering differential cross section for spheres of three different sizes and four different real refractive indices. The incident light has a wavelength of $\lambda = 532$ nm, and is polarized perpendicular to the scattering plane. The cross section has been averaged over 10° scattering angle ranges (i.e., ±5°) and plotted versus the middle angle. Particle diameters, $D = 2R$, are labeled.

Figure 1 shows the angular dependence of the differential scattering cross sections for three different particle diameters and four different real refractive indices calculated using an online Mie program [12]. These plots have been averaged over a range of 10° at each angle. Thus, if the scattering angle is 37°, the plotted differential cross section is the result of averaging the cross sections calculated from angles 32° to 42° at 1° intervals. This removes the ripple structure with spacing $\sim\lambda/2R$.

Figure 1 demonstrates the stationary angle for the real part of the refractive index at 37°. Remember, this includes the angle range ±5°. It is also interesting to remember that for particles this large, the total scattering cross section is very nearly $2\pi R^2$. Thus, one might surmise that since the total scattering is the integral over all space, i.e., over all 4π steradians, the stationary angle results from scattering shifting between angles while the total remains constant.

Figure 2 demonstrates the stationary angle for the imaginary part of the refractive index characterized by κkR. As for Fig. 1, this includes the angle range ±5°. This stationary angle is more of a range and not particular stationary. It lies in the region of ~90° to 140°, the average of which is a nominal value of 115°. While imperfect, the functionality on κkR abates in this angular range.

Figure 3 takes another perspective on stationary angles. There, we see that the real part stationary angle at 37° is lost when $\kappa kR = 3$. This is the saturation value, which means larger values have no more effect. The imaginary part stationary region exists in a semi-quantitative manner, as indicated by the arrows in the figure.

Despite the stationary angle imperfections, they do indicate regions where the differential scattering cross section has either no or a weak dependence on one or the other of the two parts of the complex refractive index. Thus, we will not lament the imperfections, but rather see if these angles can ease the pain of measuring the complex index of refraction.

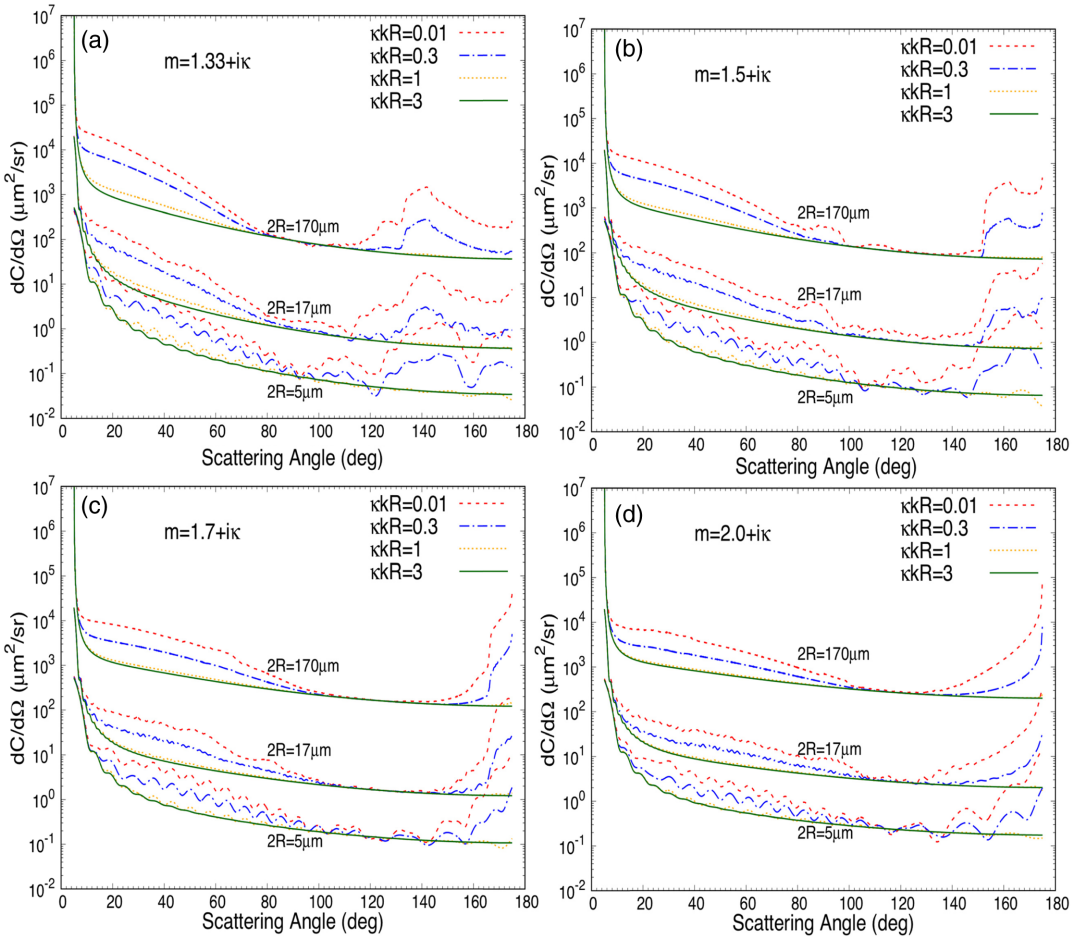

Fig. 2. Light scattering differential cross section for spheres of three different sizes, four different real refractive indices, and four different values of the parameter $\kappa k R$. The incident light has a wavelength of $\lambda = 532$ nm and is polarized perpendicular to the scattering plane. The cross section has been averaged over 10° scattering angle ranges (i.e., ±5°) and plotted versus the middle angle. Particle diameters, $D = 2R$, are labeled.

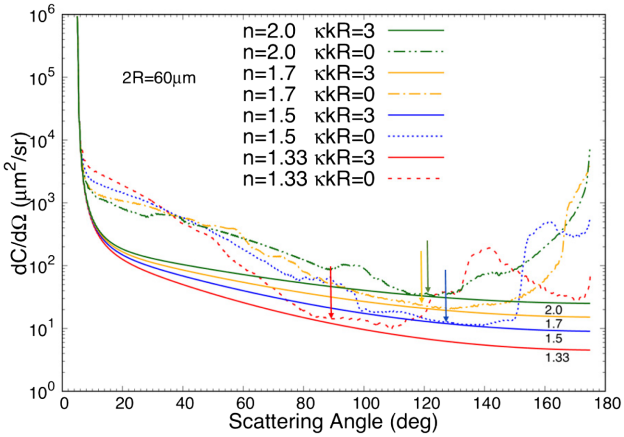

Fig. 3. Light scattering differential cross section for a $2R = 60$ μm diameter sphere of four different real refractive indices coupled with extremes of the parameter $\kappa k R = 0$ (no effect of κ) and $\kappa k R = 3$ (saturated effect of κ). The incident light has a wavelength of $\lambda = 532$ nm and is polarized perpendicular to the scattering plane. The cross section has been averaged over 10° scattering angle ranges (i.e., ±5°) and plotted versus the middle angle. Arrows indicate rough stationary angles for imaginary refractive index κ.

3. EXPERIMENTAL MEASUREMENTS AND ANALYSIS

In order to validate the concept of a three-detector device using the two stationary angles, experiments were conducted. In these experiments, scattered light intensities of droplets of nigrosine dye solutions in water and toluene at different concentrations were measured for the three different scattering angles. Nigrosine was chosen because the optical absorbance of its solutions does not have a significant wavelength dependence; hence, the solutions are gray or black.

For the complex refractive index of the nigrosine–water and nigrosine–toluene solutions, it was assumed that the real part was the same as the neat solvents. This n is 1.33 for water and 1.497 for toluene. This is justified because the molar concentrations of the dye were quite small. The imaginary part of the refractive index, κ, was determined experimentally as a function of nigrosine concentration by measuring the absorbance of bulk solutions held in thin cuvettes. The Lambert–Beer law for absorbance is

$$I(x) = I(0)\exp(-2\kappa k x), \tag{2}$$

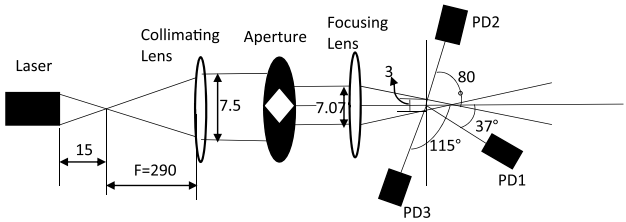

Fig. 4. Schematic diagram of light-scattering experimental setup, dimensions (mm).

where x is the optical path length in the cuvette and $k = 2\pi/\lambda$. Note that the thinness of the cuvettes for the bulk measurement has to be comparable to the size of the droplets to be measured because both are controlled by the relative skin depth parameter κkR or κkx. We found linear dependencies of κ with the dye concentration that included $\kappa = 0$ when the concentration was zero.

A schematic diagram of the experimental light-scattering setup is shown in Fig. 4. Similar to our previous work, it used a 5 mW, 532 nm wavelength laser for the light source. The polarization was vertical, perpendicular to the scattering plane. The beam was expanded to a waist of 7.5 mm. It then passed through a diamond-shaped aperture to create a diamond-shaped beam with vertical and horizontal diagonals. This beam then passed through a focusing lens on the way to the scattering volume, where it had a diamond shape with 3 mm diagonals.

A syringe with a 36G beveled-shape needle (35 μm inner diameter and 120 μm outer diameter) was used to make droplets of the nigrosine–water or nigrosine–toluene solution. The size of the droplets was measured under a microscope as they were hanging from the needle tip before they were released to fall through the scattering volume. The fall distance to the scattering volume was 1.2 cm. Assuming the droplets fall with the acceleration of gravity independent of their size, Newtonian kinematics leads to the average velocity through the scattering volume to be 0.485 mm/msec and the time to pass through the scattering volume as about 6 msec.

Scattered light was detected by three photodiodes. These photodiodes were compared to each other and found to have essentially identical sensitivities. Two were positioned at the stationary angles 37° and 115°, and the third at 80°. This third angle was chosen based on the scattering having robust and monotonic behavior with the two parts of the complex refractive index. The photodiodes were positioned at identical distances, and thus had identical solid angles from the center of the beam with an angular spread of 10°. These photodiodes recorded instantaneously the scattered light intensity and time of flight for each droplet as they fell through the diamond-shaped beam. As described in our previous work [7], this important feature allowed us to know when a droplet fell through the center of the beam, as indicated by the longest illumination time. Then the droplet was at equal distance from all three identical detectors.

To determine the droplet primary properties of size R and refractive index $m = n + i\kappa$ using scattering at the three chosen angles, an iterative numerical procedure was developed. Actual differential scattering cross sections for a variety of sizes ($2R = 5$, 17, and 170 μm) and refractive indices ($n = 1.33$, 1.5, 1.7, 2) and ($\kappa kR = 0.01$, 0.3, 1, 3) were obtained using an online Mie program [12]. Using these actual values of $dC/d\Omega$, polynomial fit equations were found for the differential scattering cross section as a function of the particle size and refractive index for the three aforementioned scattering angles. These results are

$$dC/d\Omega\,(37^\circ) = \left[\frac{0.672}{30 * (\kappa kR)^2 + 1} + 0.048\right] R^2 \quad \textbf{(3)}$$

$$dC/d\Omega\,(80^\circ) = [-0.0224(n-0.33)^2 + 0.124(n-0.33) - 0.0932]R^2(\kappa kR)^{-0.38} \quad \textbf{(4)}$$

$$dC/d\Omega\,(115^\circ) = 0.0474(n-1)^{1.4}R^{1.9}. \quad \textbf{(5)}$$

Equations (3)–(5) are an inversion iteration to invert light scattering data to the particle properties. They can be solved simultaneously and iteratively to determine size R of the particle, κkR, and the real part n of the refractive index. Once κkR and R have been determined, one can simply calculate κ. To iteratively solve the non-linear system of equations, the well-known Newton's method of iteration was used.

4. RESULTS AND DISCUSSION

To test our method for inversion of the light scattering data to the three primary properties of the spherical droplets, R, n, and κ using Eqs. (3)–(5), experiments were performed on two sets of liquid droplets. One used droplets of solutions of nigrosine in water with known n and measured κ that were $2R = 300 \pm 10$ μm in diameter; the other used droplets of the solutions of nigrosine in toluene again, with known n and measured κ that were $2R = 220 \pm 10$ μm in diameter. We will call the size measure with the microscope and the bulk measurements of the refractive index the "actual" values.

The droplets fell through the diamond-shaped beam for a time of several milliseconds, and the peak values of the output voltage were recorded. This was done ten times and then averaged. These averages were used in the inversion equations, Eqs. (3)–(5), to iteratively solve for the droplet diameter, $2R$, n, and κkR. Then, the measured and the actual values were compared as summarized in Table 1. At most, it took six iterations for the inversion to converge.

The same experiments and calculations were repeated for the droplets of the solutions of nigrosine in toluene with 220 ± 10 μm diameter of known n and κ to check for the validity of our models for a different material with a different refractive index. The results are shown in Table 2.

The results in Tables 1 and 2 show mostly a few to several percent discrepancies between the actual (bulk) values of size and real refractive index, and those measured via the light-scattering method developed here. Deviations for the skin depth parameter, κkR, range from several percent to as much as 20%.

This experiment was limited to large droplets, and we were not able to handle smaller ones. Therefore, to test the inversion iteration of Eqs. (3)–(5), we performed a theoretical study with a set of particle sizes and refractive indices rather randomly picked from the range of size parameters for which we expect our

Table 1. Comparison of Actual to Measured Values of Droplet Diameter $2R$, κkR, and n for Nigrosine Solution in Water[a]

$2R_{actual}$ (± 10 μm)	$2R_{meas}$ (μm)	$\kappa k R_{actual}$ ($\pm 9\%$)	$\kappa k R_{meas}$	n_{actual}	n_{meas}	Discrepancy (%) $2R$	κkR	n
300	286	0.89	0.72	1.33	1.34	−5	−19	+0.75
300	287	0.89	0.71	1.33	1.33	−4	−20	0
300	276	0.89	0.75	1.33	1.34	−8	−16	+0.75
300	289	0.89	0.73	1.33	1.33	−4	−18	0
300	286	0.89	0.73	1.33	1.32	−5	−18	−0.75
300	292	0.77	0.61	1.33	1.31	−3	−20	−1.5
300	297	0.77	0.62	1.33	1.31	−1	−19	−1.5
300	274	0.77	0.68	1.33	1.32	−9	−12	−0.75
300	273	0.77	0.65	1.33	1.32	−9	−15	−0.75
300	292	0.77	0.61	1.33	1.31	−3	−20	−1.5

[a]Percent discrepancies between actual and measured are given in the right hand columns.

Table 2. Comparison of Actual to Measured Values of Droplet Diameter, $2R$, κkR, and n for Nigrosine Solution in Toluene[a]

$2R_{actual}$ (± 10 μm)	$2R_{meas}$ (μm)	$\kappa k R_{actual}$ ($\pm 9\%$)	$\kappa k R_{meas}$	n_{actual}	n_{meas}	Discrepancy (%) $2R$	κkR	n
220	223	0.80	0.70	1.49	1.41	+1	−12	−5
220	228	0.80	0.74	1.49	1.40	+4	−7	−6
220	215	0.80	0.74	1.49	1.40	−2	−7	−6
220	217	0.80	0.74	1.49	1.43	−1	−7	−4
220	219	0.80	0.71	1.49	1.41	−0.5	−11	−6
220	208	1.10	1.0	1.49	1.44	−5	−9	−3
220	218	1.10	1.19	1.49	1.43	−1	+8	−4
220	214	1.10	1.20	1.49	1.45	−3	+9	−3
220	205	1.10	1.24	1.49	1.49	−7	+13	0
220	210	1.10	1.18	1.49	1.46	−4	+7	−2

[a]Percent discrepancies between actual and measured are given in the righthand columns.

approach to be valid. This set is given in Table 3 as "actual" values. The Mie theory was used to calculate the differential cross sections of the particles in this set. These cross sections were used to find a total scattering for the angles $37° \pm 5°$, $80° \pm 5°$, and $115° \pm 5°$. This simulates the need to detect light over these ranges of angles. These three total scatterings were then used as inputs to the iterative approach of Eqs. (3)–(5) to give an output measured, "meas" values, also given in Table 3. The results show that size, the diameter $2R$, can be extracted quite well, to a few percent, by the iteration. It begins to fail when $2R < 10$ μm as expected. The real refractive index is also measured well to a few percent. The biggest discrepancies involve the imaginary part of the refractive index as described by κkR, where we find systematic trends to measure too small by 10% to 20%. These results are very consistent with those in Tables 1 and 2.

Table 3. Theoretical Test of our Iterative Inversion Approach Embodied in Eqs. (3), (4), and (5)[a,b,c]

$2R_{actual}$ (± 10 μm)	$2R_{meas}$ (μm)	$\kappa k R_{actual}$ ($\pm 9\%$)	$\kappa k R_{meas}$	n_{actual}	n_{meas}	Discrepancy (%) $2R$	κkR	n
5	5.8	0.21	0.19	1.44	1.39	16	−11	−3.6
10	9.8	0.14	0.115	1.53	1.54	−2	−18	0.6
10	9.9	0.06	0.046	1.56	1.59	−1	−23	1.9
20	19	0.12	0.10	1.56	1.57	−4	−15	0.6
50	52	0.40	0.33	1.70	1.61	4	−18	−5.5
50	52.5	0.40	0.33	1.50	1.43	5	−18	−5.0
100	102	1.00	0.92	1.60	1.56	2	−8	−2.6
100	96	0.10	0.092	1.60	1.59	−4	−8	−0.6
100	101	0.30	0.28	1.60	1.56	1	−6	−2.6
110	107	1.56	1.65	1.53	1.50	−3	6	−2.0

[a]The Mie equations were applied to spheres with "actual" values of size, $2R$, κkR, and the real part of the refractive index, n, to yield scattering data.
[b]The inversion of these data yielded the measured values, designated by "meas".
[c]Percent discrepancies between actual and measured are given in the right hand columns.

5. CONCLUSIONS

We demonstrated that for spherical particles greater than ca. 5 μm, the differential scattering cross section has "stationary angles" where the scattering is only weakly dependent on the real and imaginary parts of the refractive index ($m = n + i\kappa$) when integrated over angle ranges near $37 \pm 5°$ and $115 \pm 5°$, respectively. We used this fact to construct a simple optical setup which could determine the size and complex index of refraction of large, single, spherical particles simultaneously by measuring the scattered light intensity of particles at three different scattering angle ranges of $37 \pm 5°$, $80 \pm 5°$, and $115 \pm 5°$. To validate this research, we tested our setup with 300 μm diameter droplets of nigrosine–water solutions and 220 μm diameter droplets of nigrosine–toluene solutions. The setup measured values agreed well with the actual values determined by bulk means. We also tested our inversion iteration on simulated data over a diameter range of 5 to 110 μm with similar success.

Funding. National Science Foundation (AGM 1649783).

Acknowledgment. We thank J. B. Maughan for help with plotting some of the figures.

Disclosures. The authors declare no conflicts of interest.

REFERENCES

1. M. Kerker, *The Scattering of Light, and Other Electromagnetic Radiation* (Academic, 1969).
2. T. Eidhammer, D. C. Montague, and T. Deshler, "Determination of index of refraction and size of supermicrometer particles from light scattering measurements at two angles," J. Geophys. Res. Atmos. **113**(D16), D16206 (2008).
3. D. Baumgardner, J. E. Dye, B. Gandrud, K. Barr, K. Kelly, and K. R. Chan, "Refractive indices of aerosols in the upper troposphere and lower stratosphere," Geophys. Res. Lett. **23**, 749–752 (1996).
4. H. L. Hu, X. B. Li, Y. C. Zhang, and T. Li, "Determination of the refractive index and size distribution of aerosol from dual-scattering-angle optical particle counter measurements," Appl. Opt. **45**, 3864–3870 (2006).
5. W. W. Szymanski, A. Nagy, A. Czitrovszky, and P. Jani, "A new method for the simultaneous measurement of aerosol particle size, complex refractive index and particle density," Meas. Sci. Technol. **13**, 303–307 (2002).
6. A. Nagy, W. W. Szymanski, P. Gal, A. Golczewski, and A. Czitrovszky, "Numerical and experimental study of the performance of the dual wavelength optical particle spectrometer (DWOPS)," J. Aerosol. Sci. **38**, 467–478 (2007).
7. M. S. Waez, S. J. Eckels, and C. M. Sorensen, "A refractive-index and position-independent single-particle detector for large, nonabsorbing, spherical particles," Aerosol Sci. Technol. **52**, 1429–1436 (2018).
8. C. M. Sorensen, "Q-space analysis of scattering by particles: a review," J. Quant. Spectrosc. Radiat. Transfer **131**, 3–12 (2013).
9. G. Wang, A. Chakrabarti, and C. M. Sorensen, "Effect of the imaginary part of the refractive index on light scattering by spheres," J. Opt. Soc. Am. A **32**, 1231–1235 (2015).
10. C. M. Sorensen, J. B. Maughan, and H. Moosmuller, "Spherical particle absorption over a broad range of imaginary refractive index," J. Quant. Spectrosc. Radiat. Transfer **226**, 81–86 (2019).
11. J. B. Maughan and C. M. Sorensen, "Universal parameter to describe the reduction of refraction effects in the scattering of absorbing spheres," J. Opt. Soc. Am. A **37**, 1456–1464 (2020).
12. P. Laven, *Separating Diffraction from Scattering: The Million-Dollar Challenge* (2010).